iScience

CellPress
OPEN ACCESS

Article

Propagating motor cortical patterns of excitability are ubiquitous across human and non-human primate movement initiation

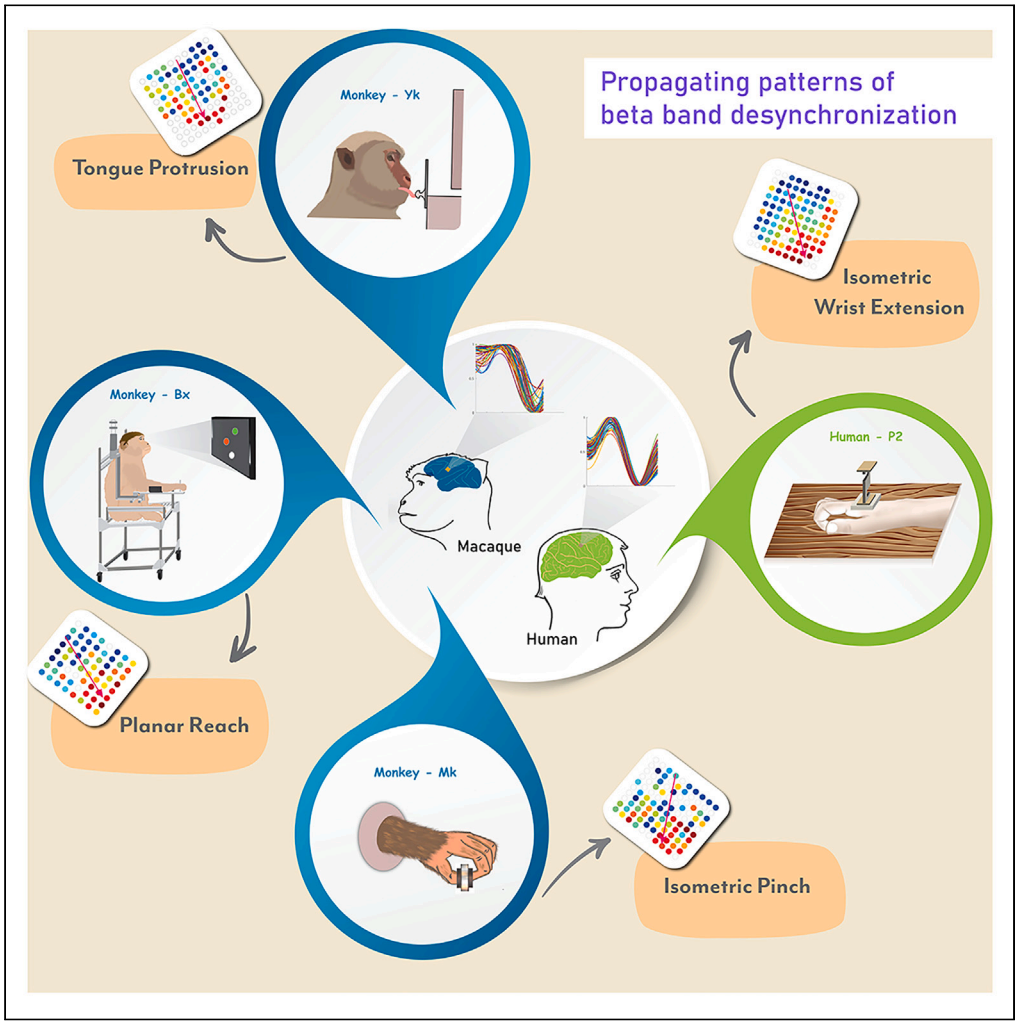

Karthikeyan Balasubramanian, Fritzie I. Arce-McShane, Brian M. Dekleva, Jennifer L. Collinger, Nicholas G. Hatsopoulos

nicho@uchicago.edu

Highlights

Propagating Patterns of excitability in M1 is generic across various motor tasks

Both human and non-human primates exhibit these propagating patterns

Such patterns appear invariant to kinematics or kinetics of the behavior

Response times are affected by the directionality of pattern propagation

Balasubramanian et al., iScience 26, 106518
April 21, 2023
https://doi.org/10.1016/j.isci.2023.106518

iScience

CellPress
OPEN ACCESS

Article

Propagating motor cortical patterns of excitability are ubiquitous across human and non-human primate movement initiation

Karthikeyan Balasubramanian,[1] Fritzie I. Arce-McShane,[1,3] Brian M. Dekleva,[4,5,7] Jennifer L. Collinger,[4,5,6,7,8,9] and Nicholas G. Hatsopoulos[1,2,10,*]

SUMMARY

A spatiotemporal pattern of excitability propagates across the primary motor cortex prior to the onset of a reaching movement in non-human primates. If this pattern is a necessary component of voluntary movement initiation, it should be present across a variety of motor tasks, end-effectors, and even species. Here, we show that propagating patterns of excitability occur during the initiation of precision grip force and tongue protrusion in non-human primates, and even isometric wrist extension in a human participant. In all tasks, the directions of propagation across the cortical sheet were bimodally distributed across trials with modes oriented roughly opposite to one another. Propagation speed was unimodally distributed with similar mean speeds across tasks and species. Additionally, propagation direction and speed did not vary systematically with any behavioral measures except response times indicating that this propagating pattern is invariant to kinematic or kinetic details and may be a generic movement initiation signal.

INTRODUCTION

Movement initiation engages large distributed patterns of activity across motor cortex (M1) that are highly overlapping across different behavioral conditions with apparently very little spatial structure aside from a crude somatotopic map along the medio-lateral axis.[1] However, we have recently shown that a pattern of excitability propagates across the arm area of M1 along a roughly rostro-caudal axis prior to the initiation of a reach movement. This pattern was determined by examining the timing of beta frequency (i.e. 15–35 Hz) oscillation attenuation in the local field potential (LFP) across electrodes.[1] Beta frequency oscillations are a hallmark of M1 as well as other motor structures including the premotor cortex, cerebellum and basal ganglia.[2–4] As other studies have shown, the amplitude of these beta oscillations attenuates at a fixed latency prior to movement initiation at a specific cortical site.[1,5–10] However, this latency varies systematically across the motor cortical sheet resulting in a propagating pattern in one of the two possible modal directions along the rostro-caudal axis.[1] Beta oscillation attenuation is considered a signature of M1 excitability because the magnitude of muscle potentials evoked by transcranial magnetic stimulation is positively correlated with the magnitude of beta oscillation attenuation in M1.[11–13]

The fact that beta oscillation attenuation latency is fixed with respect to movement initiation at any given cortical site but varies linearly with response time with respect to a go cue indicates that it is a reliable signal of movement initiation.[1,14,15] Moreover, our recent results using propagating intracortical microstimulation (ICMS) across a set of electrodes showed that response time significantly increases when propagating ICMS is delivered against, but not with, the natural propagating pattern.[1] Together, these results suggest that this propagating pattern of excitability may be a necessary component of movement initiation. To provide further evidence that this is a general feature of movement initiation, here we show that similar propagating patterns occur prior to movement onset of different motor behaviors involving different body parts and is even observed in human motor cortex during behavior.

RESULTS

Propagating beta patterns prevail across tasks and species

Three male rhesus macaques (Bx, Yk, and Mk) and one human participant (P2) performed either a movement generation or a force generation task (Figure 1, top row). Multi-unit activity and local field potentials (LFP)

[1]Department of Organismal Biology and Anatomy, University of Chicago, Chicago, IL 60637, USA

[2]Committee on Computational Neuroscience, University of Chicago, Chicago, IL 60637, USA

[3]Department of Oral Health Sciences, School of Dentistry, Graduate Program in Neuroscience, University of Washington, Seattle, WA 98195, USA

[4]Rehab Neural Engineering Labs, University of Pittsburgh, Pittsburgh, PA 15260, USA

[5]Department of Physical Medicine & Rehabilitation, University of Pittsburgh, Pittsburgh, PA 15260, USA

[6]Department of Bioengineering, University of Pittsburgh, Pittsburgh, PA 15260, USA

[7]Center for the Neural Basis of Cognition, Pittsburgh, PA 15213, USA

[8]Human Engineering Research Labs, VA Center of Excellence, Department of Veterans Affairs, Pittsburgh, PA 15260, USA

[9]Department of Biomedical Engineering, Carnegie Mellon University, Pittsburgh, PA 15213, USA

[10]Lead contact

*Correspondence: nicho@uchicago.edu

https://doi.org/10.1016/j.isci.2023.106518

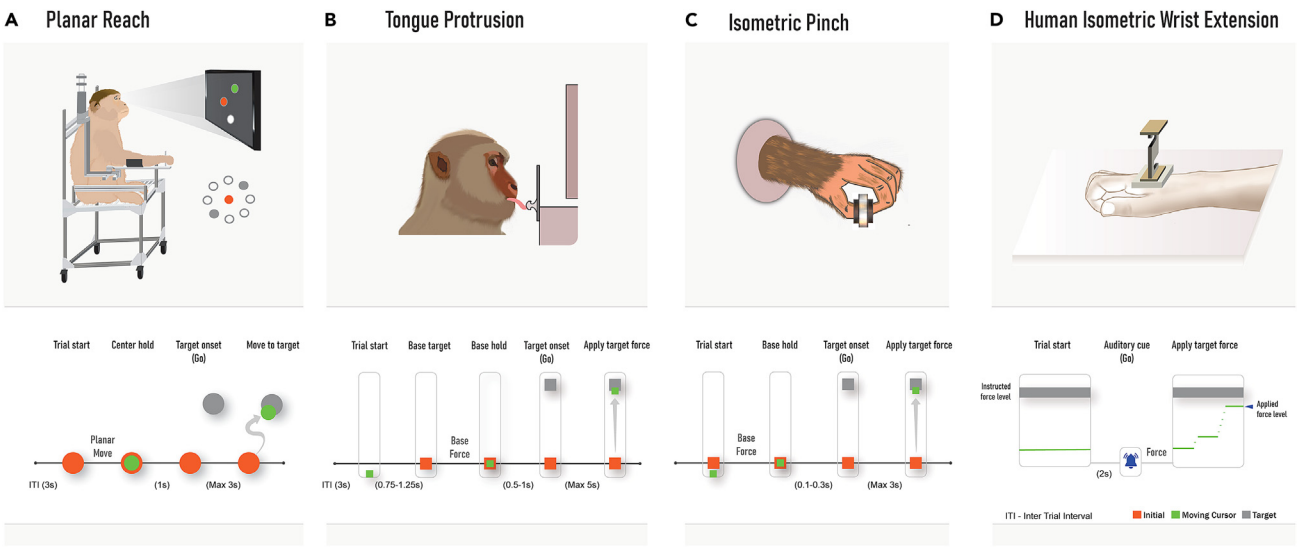

Figure 1. Schematic of the behavioral paradigm

(top row) shows schematics of animals performing (A) a planar reach, (B) tongue protrusion, (C) isometric pinch and (D) the human participant performing an isometric wrist extension behavior. (bottom row) shows the temporal sequence events associated with each of the tasks. For the planar reach, the animal moves the green cursor to the center target (orange circle). The animal holds the cursor in the center target for a fixed duration of 1 s, and one of the gray-filled targets appear as the final reach target for every trial. The animal uses the exoskeleton to move the cursor to the gray peripheral target, within a time limit of 3 s. For the tongue protrusion task, the base target (orange square) appears after a random delay of 0.75–1.25 s from the trial start. The animal applies a base force such that the green cursor reaches the base target and holds the force for a varying delay period between 0.5 and 1 s. The final gray target appears after the hold period. The animal continues to apply further force to reach the target with a time limit of 5 s. The isometric pinch task is similar to the tongue protrusion except that the appearance of the base target (orange square) marks the trial start and the animal uses the thumb and the index finger to generate force. The base hold period in this case is between 0.1 and 0.3 s, and the maximum allowable time to target is 3 s. In the human wrist extension task, the subject sees a target force level (either low or high, indicated by the position of a gray horizontal bar), and after 2 s of fixed delay, an auditory cue chimes to indicate Go. The subject applies isometric force to move the green cursor line to the target force level indicated by the gray bar. The subject is able to see the applied force levels from the past 5 s.

were simultaneously recorded using implanted electrode arrays each of which covered a portion of the motor cortex (Blackrock Neurotech Inc., Salt Lake City, Utah, USA). Monkey Bx performed planar reaching with its right upper limb in 2D space using a KINARM exoskeleton (BKIN Technologies, ON, Canada). The animal reached for visual targets presented at 45° or 225° (corresponding to movements away from and to the right of the body or toward and to the left of the body, respectively). The two target presentations were randomly interleaved within each training session. Monkey Yk was trained to perform a tongue protrusion task by applying an isometric force on a sensor that drove a cursor vertically on a computer screen, proportional to the applied force. Monkey Mk performed an isometric pinch behavior (precision grip) using the thumb and index fingers. The applied pinch force was translated into a cursor movement vertically on a screen. The human participant generated two levels (low and high) of wrist extension force under isometric conditions. The generated force drove a cursor on the computer screen, providing visual feedback. The temporal sequence of events associated with each behavior is provided in Figure 1 (bottom row).

Continuous neural signals were recorded using multi-electrode arrays implanted in the motor cortex of the species (see Figure 2, top row; see STAR Methods for additional details). Single-trial beta oscillation profiles were extracted from the LFP signals after band-passing them to a narrow band in the beta range of frequencies 31 $\pm$ 3 Hz (Bx and Mk), 23 $\pm$ 3 Hz (Yk), and 30 $\pm$ 3 Hz (P2) for the human subject, and beta amplitude envelopes were computed using the Hilbert Trans-form (Broader beta band filtering is possible but may influence the efficacy of the subsequent processing; see Data S1). The beta envelopes were de-noised using an auto-encoder (Figure 2, middle row), and the times at which these envelopes attenuated below a certain magnitude threshold were computed for each trial. These beta attenuation times (BATs) were used to compute the propagation orientation (i.e. beta attenuation orientation or BAO) using a 2D regression fit (Figure 2, bottom row) and the propagation speed using the time gradient of each trial (see STAR Methods and[1] for details). The beta frequency amplitude attenuated before movement/force onset for all four behaviors.

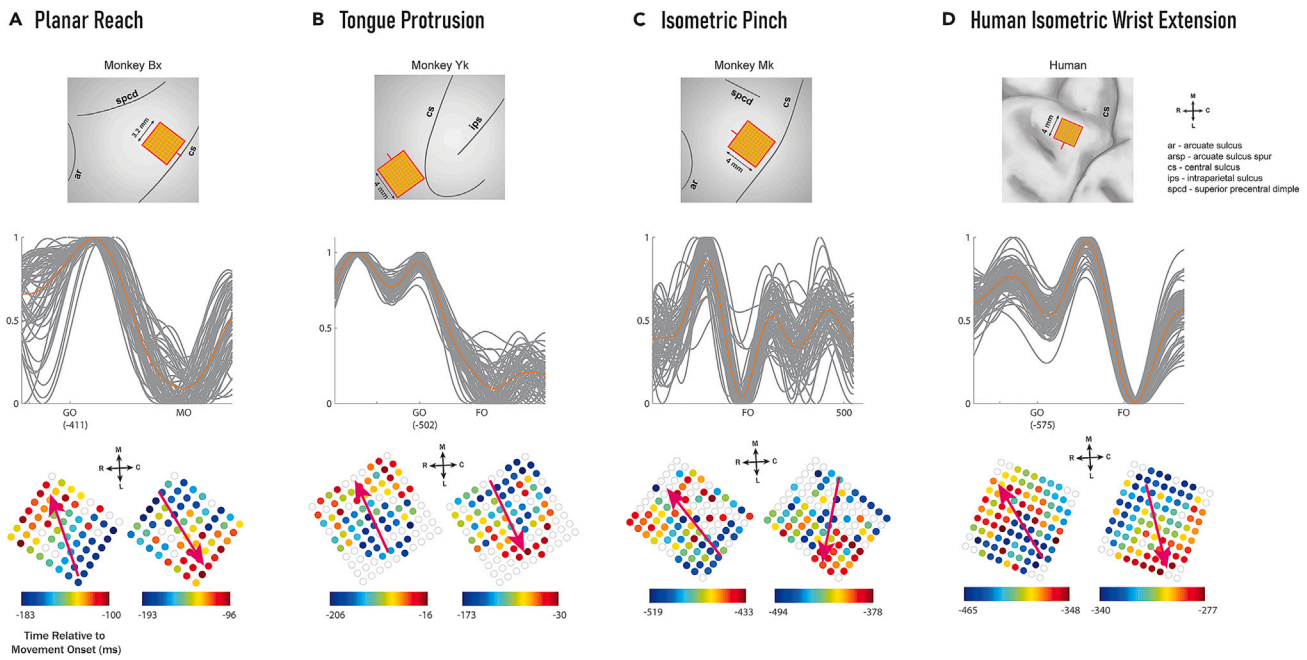

Figure 2. Propagating patterns are prevalent across a variety of motor tasks in non-human primates and humans

(top row) shows the anatomical landmarks of the motor cortex in relation to the multi-electrode array implants. (middle row) normalized beta-band envelopes recorded from a group of electrodes showing attenuation during a single trial. The envelopes are aligned to movement/force onset. The gray traces correspond to the individual electrode recordings, and the orange denotes the mean beta attenuation envelope. (bottom row) patterns of beta attenuation times propagating across the electrode grid in opposing directions (red arrows) for two different single trials. For the planar reaching, both trials were from a 45^0 target direction. Likewise, for the wrist extension behavior, the trials were from similar instructed force levels. The color scheme in the grid represents the time relative to movement/force onset at which the beta attenuated below a certain threshold on a given electrode (blue electrodes attenuated earlier than the red electrodes).

Single-trial beta propagation is predominantly bimodal

The BAOs were computed for single trials across multiple sessions, and the results were pooled for further analysis (11 sessions for Bx, 6 for Yk, 2 for Mk, and 6 for P2). Trials were chosen for further analyses based on inclusion criteria determined by a shuffling analysis (see STAR Methods; Data S2). The trials with BAO regression fit that met the R^2 inclusion criteria for each monkey were included ($R^2 \geq 0.2$ for Bx, 0.1 for Yk, Mk, and P2; 1381 out of 1823 trials (76%) for Bx, 689 out of 699 (98%) for Yk, 79 out of 90 trials (88%) for Mk, 200 out of 216 (92%) for P2). The BAO distribution was predominantly bimodal in all the behavioral tasks (Rayleigh's test for uniform distribution; p = 5.3e-9 for Bx, 3.9e-3 for Yk, 0.003 for Mk, 0.4e-5 for P2) (Figure 3A and Data S3) and roughly aligned along an axis, specifically rostromedial and caudolateral axes for Bx and Yk and medio-lateral axis for the human (P2). For Mk performing the isometric pinch task, the two modes were associated with rostromedial and lateral directions and so were not exactly opposite to one another. The distribution of BAOs was well fit by a two-mode, von-Mises model with modes pointing along 119 and 307° for Bx, 138 and 329° for Yk, 128 and 247° for Mk, and 51 and 260° for the human participant.

In addition to the propagation directions, propagation speeds were computed for each trial. The BATs and the electrode spacing of the arrays (400 μm for all the arrays) were used to compute the propagation speeds for each trial (see STAR Methods). The distribution of the propagation speeds was fitted with gamma profiles (Figure 3B). The mean propagation speed was 4.72 cm/s for the reaching task, 2.66 cm/s for the tongue protrusion task, 5.26 cm/s for the pinch behavior, and 4.62 cm/s for the human isometric wrist extension task.

Propagating patterns are condition invariant

We hypothesized that these propagating patterns of excitability signaled movement initiation in a condition-invariant fashion and did not carry information about movement type. To test this, we compared BAO

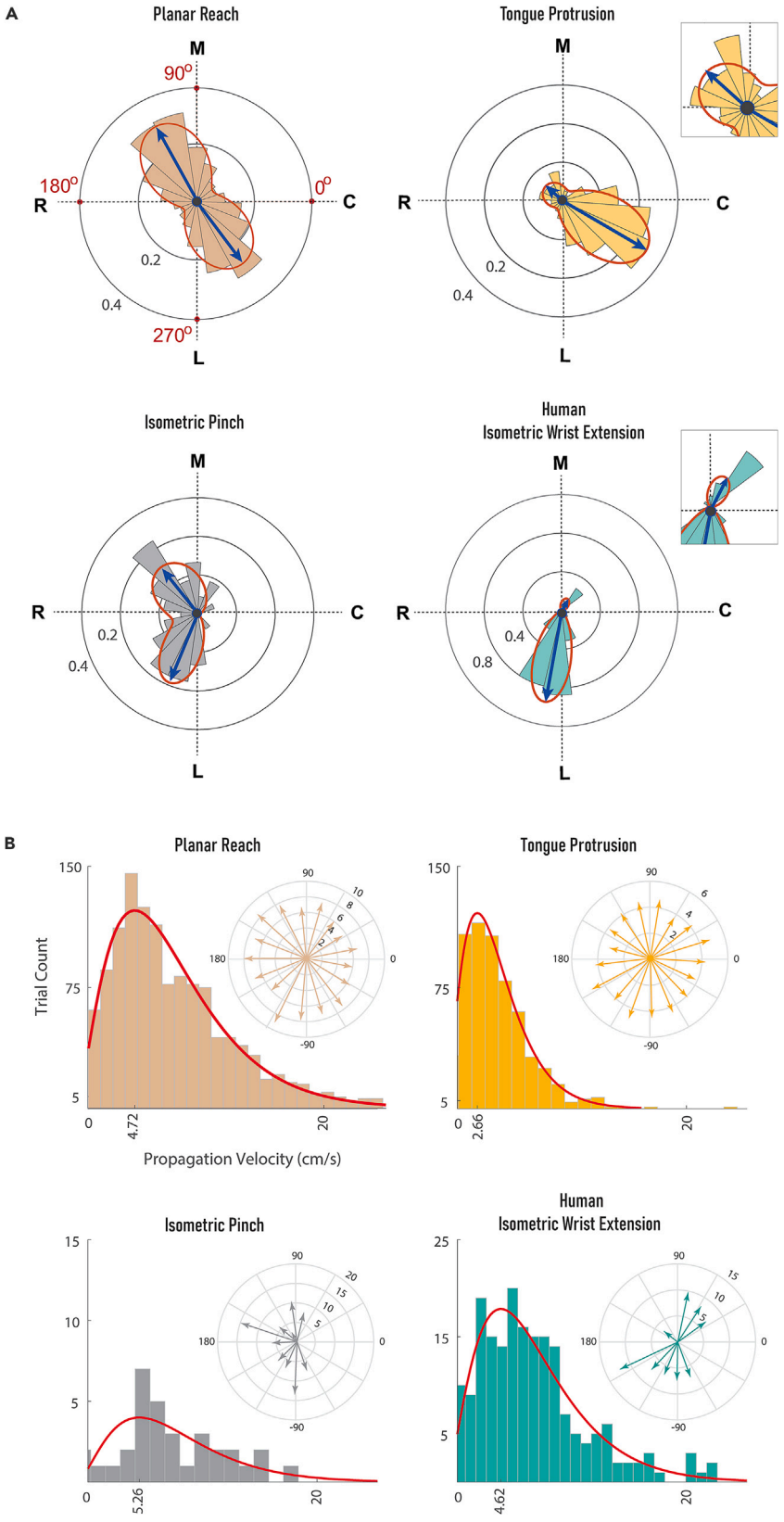
A
Planar Reach
M
90°
180°
0°
R
C
270°
L
0.2
0.4
Tongue Protrusion
Isometric Pinch
Human
Isometric Wrist Extension
0.8
B
Trial Count
150
75
5
0
4.72
20
Propagation Velocity (cm/s)
2.66
15
10
5.26
25
4.62

Figure 3. Beta attenuation times propagate along two primary directions with comparable velocities

(A) The propagation direction (in angles) of beta attenuation followed a bimodal distribution. The red trace denotes von Mises fits of the BAO distribution for each task. Blue pointed arrows show the two primary modes of the fitted model. Non-human primates that performed planar reach (monkey Bx), tongue protrusion (monkey Yk), and isometric pinch (monkey Mk) had BAO modes pointing along [140 and −32°], [174 and −17°], and [157 and −84°] respectively. The wrist extension task (P2) showed BAO modes along [-174 and 23°] (degrees are rounded to integers). Insets for the tongue protrusion and isometric wrist extension tasks are close-ups of the distributions of propagation directions to emphasize that the distributions were bimodal.

(B) Propagation velocity histograms fitted with a gamma distribution, and the mean velocities denoted. The mean propagation velocities were 4.72 cm/s for the planar reach, 2.66 for the tongue protrusion, 5.26 for the isometric pinch, and 4.62 for the isometric wrist extension. Inset shows mean propagation speeds grouped by trials propagating along a given direction. The absence of trials in a given BAO direction resulted in a mean speed equal to zero in that direction.

distributions and propagation speeds across different task conditions within reaching and isometric wrist extension behaviors. For monkey Bx, the BAO distributions for the two different reach directions remained bimodal (Figure 3A, top), with modes along 120 and 307° for a 45° reach away from the body, and 123 and 306° for a 225° reach toward the body. Moreover, the distributions did not differ significantly ($p = 0.2$; Kuiper's two-sample test). Likewise, the mean propagation speeds of the beta patterns remained comparable and were not statistically different ($p = 0.12$; Mann Whitney U test, Figure 3A, bottom). For reach trials moving to 45°, the patterns propagated at a speed of 4.46 cm/s as compared to 5.08 cm/s for reach trials moving to 225°.

Similar to the reaching task, the wrist extension task performed by the human participant had two conditions, i.e., trials with low and high force. Neither BAO distributions (Figure 4B, top) nor propagation speeds (Figure 4B, bottom) were statistically different for the two levels of applied forces ($p = 0.1$; Kuiper's two-sample test for the BAO distributions; $p = 0.2$; Mann Whitney U test for the propagation speeds). For the low force trials, the BAO modes were at 77 and 259° whereas the high force trials had modes at 58 and 258°. The patterns propagated at a mean speed of 4.86 cm/s and 4.36 cm/s for the low and high force conditions, respectively.

Direction of propagation affects response times

While the beta propagation properties remained invariant across kinematic and kinetic conditions, response time did differ across propagation directions. To test this, two groups of trials were formed based on their alignment with the mean modes of the von Mises fits. Trials falling within the mean ± 1 standard deviation (S.D. is equivalent to $1/\kappa$, which is the spread factor of von Mises fit) range were grouped, and their mean response times were computed. The fraction of trials selected for the response time computation is as follows: Planar Reach – 1055/1381, Tongue Protrusion – 447/689, and Human Wrist Extension – 128/200. Trials associated with beta attenuation patterns propagating in the approximate caudal direction for the non-human primates and medial direction for the human subject had significantly shorter response times as compared to patterns propagating in the opposite direction in the three tasks in which response times could be computed (i.e. tasks with a go cue) (Figure 5). The response time distributions for these three tasks are given in Data S4.

Mean response times for trials grouped by the propagation direction for planar reach were 390 ms and 400 ms in the caudo-lateral and rostro-medial directions, respectively (two-sample t-test; $p = 0.015$). For the tongue protrusion task, mean response time was 584 ms in the caudo-lateral direction and 620 ms in the opposite direction ($p = 0.0329$). Lastly, the mean response times for the wrist extension task were 785 ms in the medial direction and 840 ms in the opposite direction ($p = 0.0115$). The mean response times for the pinch task were not computed due to the lack of a go cue. We also computed mean peak reach speed and mean time to peak reach speed during the reach task associated with two propagating modes and found no statistically significant difference (two-sample t-test; $p = 0.2271$ and 0.4992). Likewise, mean peak applied force and mean time to peak applied force in the tongue protrusion, pinch force, and wrist extension tasks did not differ across the two propagating modes ($p = 0.052$ and 0.6738 for Yk, 0.06 and 0.353 for Mk, $p = 0.6545$ and 0.6636 for P2). We, however, found a small difference in the peak beta power across the two propagating directions (see Data S5). Nevertheless, the peak beta frequency did not differ. Finally, we found no statistical difference (except for Mk) in propagation speed across the two modes for all four tasks (Mann Whitney U test; $p = 0.6168$ for Bx, 0.0763 for Yk, 0.0216 for Mk, and 0.338 for P2). Moreover,

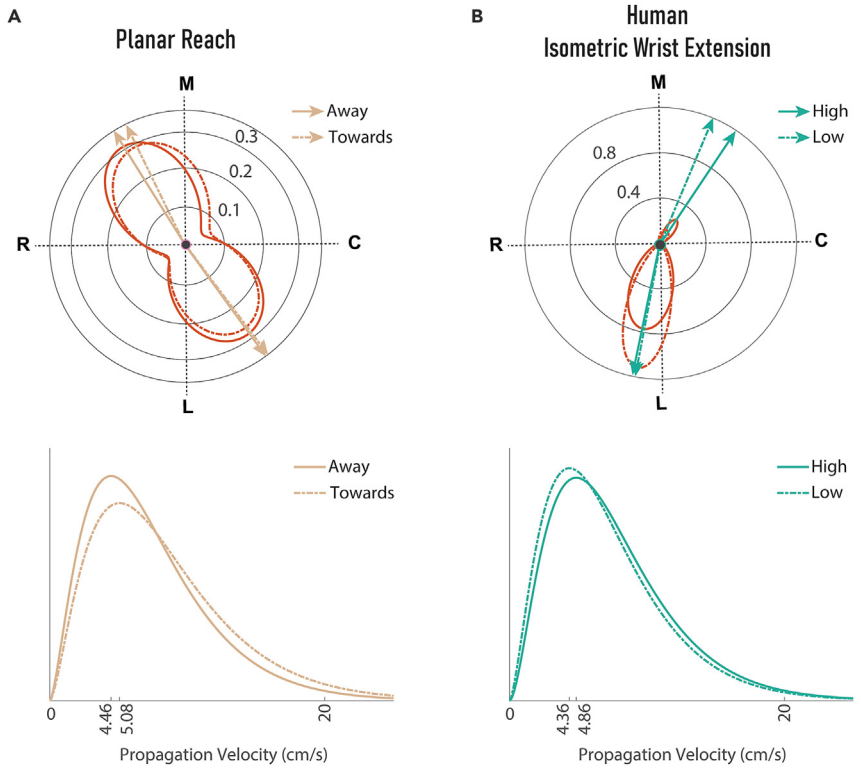

Figure 4. Propagating patterns show condition invariance

(A, top) Von-Mises fits of BAO distributions associated with 45° (solid red trace) and 225° (dotted red curves) reach targets along with the mean propagation directions of their modes (arrows) from Bx. (A, bottom) Gamma fits the propagation speeds associated with the two reach targets.

(B, top) Von-Mises fits of BAO distributions associated with high (solid trace) and low (dotted trace) force levels during the isometric wrist extension task.

(B, bottom) Gamma fits to the propagations speeds for the two force levels.

the response time showed no correlation with the movement time (see Data S6) as well as the propagation speed (Data S7).

DISCUSSION

The current study extends our previous work on propagating patterns of cortical excitability associated with movement initiation in three important ways. First, we have shown that this propagating pattern represents a general phenomenon that occurs prior to movement initiation across different end-effectors (arm, wrist, finger, and tongue), different tasks (movement and isometric force), and even different species (macaque monkeys and humans). In all cases, these patterns propagated in one of the two directions, albeit not always with equal frequency, depending on the particular trial. Moreover, the propagating speed was unimodally distributed with comparable average values (~3–5 cm/s) across all cases. The ubiquity of these propagating patterns of excitability across body parts and tasks suggests that this the spatiotemporal pattern represents a common functional property of the motor cortex associated with the initiation of all movements.

The rostro-caudal axis and speed of propagation are consistent with known properties of horizontal connectivity in monkey M1 and thus may be mediated by intrinsic M1 connectivity. Anatomical and physiological studies in non-human primate M1 have documented anisotropies in horizontal connectivity indicating a bias along the rostro-caudal axis.[16–18] In addition, the relatively slow propagation speeds are comparable with reported conduction velocities in horizontal connectivity in rodent motor cortex as well as other cortical areas mediated by presumed unmyelinated axons.[19–21] There may also be a functional reason why these patterns propagate roughly along a rostro-caudal axis. Given that the somatotopic gradient from proximal to distal representations follows a medio-lateral orientation, these propagating patterns

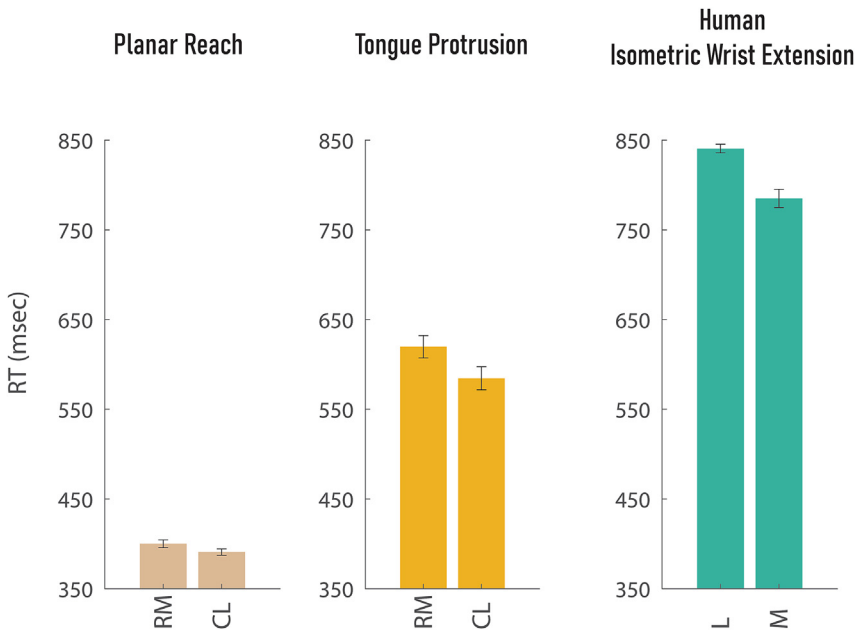

Figure 5. Response time differs across propagation direction

Trials grouped according to the two modes of propagation showed statistically significant differences in their mean response times. Trials with BAOs propagating in the caudo-lateral direction toward the central sulcus for the monkeys exhibited shorter response times and trials propagating in the medial direction for the human exhibited shorter response times. Error bars represent standard errors of the mean.

of excitability would ensure that all representations of the upper limb are synchronously in a high state of excitability.[1] However, the medio-lateral propagation axis in the human motor cortex seems inconsistent with this hypothesis given the apparent medio-lateral somatotopic gradient of the upper limb area of motor cortex based on fMRI[22] (Meier et al., 2008). Interestingly, propagating phase waves in the beta frequency range have previously been shown to also propagate medio-laterally in the motor cortex of a spinal-cord injured human whereas they propagate rostro-caudally in the macaque monkey[23–25] which suggests there may be anatomical differences in horizontal connectivity between the two species. Alternatively, the difference may be due to the spinal-cord injury of the human subjects.

Second, the properties of these propagating patterns remained invariant across different kinematic and kinetic conditions. In particular, the distributions of propagating direction and speed did not vary with reach direction (Bx) nor on instructed wrist force level (P2). A previous study has examined an "untuned," condition-invariant signal (CIS) in M1 population responses that occurs at movement initiation near the transition from preparation to execution.[26,27] This CIS is quite large and often accounts for the majority of neural variance, and the onset of this CIS can accurately predict reaction time on a trial by trial basis.[27] The propagating patterns we have observed share the condition-invariant property of the CIS documented by Kaufman and colleagues. Moreover, we have shown previously that the timing of beta oscillation attenuation correlates strongly with reaction time (see Figure 1D of[1]) So both phenomena likely arise from a common source such as input to M1 that triggers movement initiation. In fact, modeling work has suggested that a condition-invariant response in M1 emerges when an external input triggers movement initiation.[28] However, the two phenomena reflect distinct population responses in M1. The CIS reflects the spiking responses of a population of individual M1 neurons and represents a neural trajectory in an abstract state space. In contrast, the propagating patterns we have observed represent a mesoscopic description of motor cortical excitability as revealed by the attenuation of the local field potential amplitude in the beta frequency range and explicitly considers physical space on the cortical sheet. We thus argue that a complete description of M1 dynamics that occurs during the transition from preparation to execution should consider both.

Third, we have shown that response time is significantly shorter on trials exhibiting a pattern that propagates in the caudo-lateral direction for reaching and tongue protrusion in the monkey and in the medial

direction for humans as compared to the opposite directions. It is not obvious why we would observe this response time difference. One possibility is that the different directions of propagation are triggered from different input sources to M1 at movement initiation. In the case of non-human primates, inputs from the premotor cortex target more rostral regions of M1 whereas inputs from area 5 in the posterior parietal cortex (PPC) target more caudal parts of M1.[29] Thus, inputs from the premotor cortex may initiate a "wave" of excitability that begins at the rostral end of M1 whereas inputs from PPC could initiate a propagating pattern that originates in caudal M1. Response time is known to be inversely related to the planning duration, and premotor cortex is known to carry planning-related activity whose strength is inversely related to response time (Hatsopoulos et al., 2004[30]; Riehle et al., 1997[31]; Dekleva et al., 2018). Thus, we speculate that pre-planned movements may be initiated by rostral inputs entering M1 from the premotor cortex leading to rostro-to-caudal propagation and shorter response times whereas unplanned or low vigilant state movements that result in slower reaction time movements may be initiated by caudal inputs entering M1 from PPC leading to caudal-to-rostral propagation. In the case of human, it is not at all clear why trials associated with medially directed propagation would lead to shorter reaction times.

It should be noted that the spatial coverage of the electrode arrays is limited and does not encompass the entire motor cortex. Within this limited coverage, we could fit the timing of beta attenuation across the array as planar propagation patterns. However, these may be part of larger, global patterns that are more complex in nature such as radial, circular, or spiral patterns.

Two interrelated questions, however, remain unresolved. First, what functional role does a propagating pattern of excitability play in movement initiation? and, second, what makes the stereotyped propagation axis so special? To address these questions, one possibility is to examine the downstream effects of these cortical patterns on muscle recruitment. Future experiments may lead to insights into the exact role of these cortical patterns in generating muscle activity for movement initiation.

Limitations of the study

1. The implanted electrodes have limited spatial coverage on the brain. Hence, the possibility that the propagating patterns observed here could be part of a larger pattern in the brain cannot be discounted. Likewise, due to variations in the cortical thickness, the recording layer cannot be ascertained but can only be estimated between layers 3 and 5 of the motor cortex.
2. The human subject used in this study was a spinal cord injured patient. Hence, the motor cortex may have differences from a healthy subject.

STAR★METHODS

Detailed methods are provided in the online version of this paper and include the following:

- KEY RESOURCES TABLE
- RESOURCE AVAILABILITY
  - Lead contact
  - Materials availability
  - Data and code availability
- EXPERIMENTAL MODEL AND SUBJECT DETAILS
  - Behavioral tasks
  - Electrophysiology
- METHOD DETAILS
  - Beta band and single-trial beta attenuation orientation
  - Computing propagation speed
  - Computing response times of single trials
  - Shuffling analysis
- QUANTIFICATION AND STATISTICAL ANALYSIS
- ADDITIONAL RESOURCES

SUPPLEMENTAL INFORMATION

Supplemental information can be found online at https://doi.org/10.1016/j.isci.2023.106518.

ACKNOWLEDGMENTS

We would like to thank Carrie Anne Balcer and Rebecca Junod for assistance in animal care and training as well as Callum Ross, Kai Qian, and John Downey. This work was supported by the National Institute of Neurological Disorders and Stroke at the National Institutes of Health (Grants R01 NS045853, R01 NS111982 to N.G.H. and UH3NS107714 to J.L.C.). The content is solely the responsibility of the authors and does not necessarily represent the official views of the National Institutes of Health. This work used the Beagle supercomputer resources provided by the Computation Institute and the Biological Sciences Division of the University of Chicago and Argonne National Laboratory, and the Midway cluster at the Research Computing Center of the University of Chicago.

AUTHOR CONTRIBUTIONS

K.B. contributed to the conceptualization, writing and editing the article, and performed all data analyses. N.G.H. contributed to the conceptualization, non-human primate surgical procedures, and writing and editing the article. F.I.A. provided non-human primate tongue data and contributed to editing the article. B.M.D. and J.L.C. provided the human data and contributed to editing the article.

DECLARATION OF INTERESTS

N.G.H. serves as a consultant for BlackRock Neurotech, Inc., the company that sells the multi-electrode arrays and data acquisition system used in this study.

Received: May 9, 2022
Revised: November 17, 2022
Accepted: March 27, 2023
Published: March 29, 2023

REFERENCES

1. Balasubramanian, K., Papadourakis, V., Liang, W., Takahashi, K., Best, M.D., Suminski, A.J., and Hatsopoulos, N.G. (2020). Propagating motor cortical dynamics facilitate movement initiation. Neuron *106*, 526–536.e4. https://doi.org/10.1016/j.neuron.2020.02.011.

2. Donoghue, J.P., Sanes, J.N., Hatsopoulos, N.G., and Gaál, G. (1998). Neural discharge and local field potential oscillations in primate motor cortex during voluntary movements. J. Neurophysiol. *79*, 159–173.

3. Murthy, V.N., and Fetz, E.E. (1992). Coherent 25- to 35-Hz oscillations in the sensorimotor cortex of awake behaving monkeys. Proc. Natl. Acad. Sci. USA *89*, 5670–5674.

4. Sanes, J.N., Donoghue, J.P., Thangaraj, V., Edelman, R.R., and Warach, S. (1995). Shared neural substrates controlling hand movements in human motor cortex. Science *268*, 1775–1777. https://doi.org/10.1126/science.7792606.

5. Baker, S.N. (2007). Oscillatory interactions between sensorimotor cortex and the periphery. Curr. Opin. Neurobiol. *17*, 649–655. https://doi.org/10.1016/j.conb.2008.01.007.

6. Baker, S.N., Olivier, E., and Lemon, R.N. (1997). Coherent oscillations in monkey motor cortex and hand muscle EMG show task-dependent modulation. J. Physiol. (Camb.) *501*, 225–241. https://doi.org/10.1111/j.1469-7793.1997.225bo.x.

7. Engel, A.K., and Fries, P. (2010). Beta-band oscillations—signalling the status quo? Curr. Opin. Neurobiol. *20*, 156–165. https://doi.org/10.1016/j.conb.2010.02.015.

8. McFarland, D.J., Miner, L.A., Vaughan, T.M., and Wolpaw, J.R. (2000). Mu and beta rhythm topographies during motor imagery and actual movements. Brain Topogr. *12*, 177–186. https://doi.org/10.1023/A:1023437823106.

9. Pfurtscheller, G. (1981). Central beta rhythm during sensorimotor activities in man. Electroencephalogr. Clin. Neurophysiol. *51*, 253–264. https://doi.org/10.1016/0013-4694(81)90139-5.

10. Sanes, J.N., and Donoghue, J.P. (1993). Oscillations in local field potentials of the primate motor cortex during voluntary movement. Proc. Natl. Acad. Sci. USA *90*, 4470–4474.

11. Schulz, H., Übelacker, T., Keil, J., Müller, N., and Weisz, N. (2014). Now I am ready—now I am not: the influence of pre-TMS oscillations and corticomuscular coherence on motor-evoked potentials. Cerebr. Cortex *24*, 1708–1719. https://doi.org/10.1093/cercor/bht024.

12. Mäki, H., and Ilmoniemi, R.J. (2010). EEG oscillations and magnetically evoked motor potentials reflect motor system excitability in overlapping neuronal populations. Clin. Neurophysiol. *121*, 492–501. https://doi.org/10.1016/j.clinph.2009.11.078.

13. Lepage, J.-F., Saint-Amour, D., and Théoret, H. (2008). EEG and neuronavigated single-pulse TMS in the study of the observation/execution matching system: are both techniques measuring the same process? J. Neurosci. Methods *175*, 17–24. https://doi.org/10.1016/j.jneumeth.2008.07.021.

14. Kühn, A.A., Williams, D., Kupsch, A., Limousin, P., Hariz, M., Schneider, G.-H., Yarrow, K., and Brown, P. (2004). Event-related beta desynchronization in human subthalamic nucleus correlates with motor performance. Brain *127*, 735–746. https://doi.org/10.1093/brain/awh106.

15. Williams, D., Kühn, A., Kupsch, A., Tijssen, M., van Bruggen, G., Speelman, H., Hotton, G., Loukas, C., and Brown, P. (2005). The relationship between oscillatory activity and motor reaction time in the parkinsonian subthalamic nucleus. Eur. J. Neurosci. *21*, 249–258. https://doi.org/10.1111/j.1460-9568.2004.03817.x.

16. Gatter, K.C., Sloper, J.J., and Powell, T.P. (1978). The intrinsic connections of the cortex of area 4 of the monkey. Brain *101*, 513–541.

17. Hao, Y., Riehle, A., and Brochier, T.G. (2016). Mapping horizontal spread of activity in monkey motor cortex using single pulse microstimulation. Front. Neural Circ. *10*, 104. https://doi.org/10.3389/fncir.2016.00104.

18. Huntley, G.W., and Jones, E.G. (1991). Relationship of intrinsic connections to forelimb movement representations in monkey motor cortex: a correlative anatomic and physiological study. J. Neurophysiol. *66*, 390–413. https://doi.org/10.1152/jn.1991.66.2.390.

19. Aroniadou, V.A., and Keller, A. (1993). The patterns and synaptic properties of horizontal intracortical connections in the rat motor cortex. J. Neurophysiol. *70*, 1553–1569.

20. Bringuier, V., Chavane, F., Glaeser, L., and Frégnac, Y. (1999). Horizontal propagation of visual activity in the synaptic integration field of area 17 neurons. Science *283*, 695–699.

21. González-Burgos, G., Barrionuevo, G., and Lewis, D.A. (2000). Horizontal synaptic connections in monkey prefrontal cortex: an in vitro electrophysiological study. Cerebr. Cortex *10*, 82–92.

22. Meier, J.D., Aflalo, T.N., Kastner, S., and Graziano, M.S.A. (2008). Complex organization of human primary motor cortex: a high-resolution fMRI study. J. Neurophysiol. *100*, 1800–1812.

23. Rubino, D., Robbins, K.A., and Hatsopoulos, N.G. (2006). Propagating waves mediate information transfer in the motor cortex. Nat. Neurosci. *9*, 1549–1557. https://doi.org/10.1038/nn1802.

24. Takahashi, K., Saleh, M., Penn, R.D., and Hatsopoulos, N.G. (2011). Propagating waves in human motor cortex. Front. Hum. Neurosci. *5*, 40. https://doi.org/10.3389/fnhum.2011.00040.

25. Takahashi, K., Kim, S., Coleman, T.P., Brown, K.A., Suminski, A.J., Best, M.D., and Hatsopoulos, N.G. (2015). Large-scale spatiotemporal spike patterning consistent with wave propagation in motor cortex. Nat. Commun. *6*, 7169.

26. Haar, S., Dinstein, I., Shelef, I., and Donchin, O. (2017). Effector-invariant movement encoding in the human motor system. J. Neurosci. *37*, 9054–9063. https://doi.org/10.1523/JNEUROSCI.1663-17.2017.

27. Kaufman, M.T., Seely, J.S., Sussillo, D., Ryu, S.I., Shenoy, K.V., and Churchland, M.M. (2016). The largest response component in the motor cortex reflects movement timing but not movement type. eneuro *3*. ENEURO.0085-16.2016. https://doi.org/10.1523/ENEURO.0085-16.2016.

28. Sussillo, D., Churchland, M.M., Kaufman, M.T., and Shenoy, K.V. (2015). A neural network that finds a naturalistic solution for the production of muscle activity. Nat. Neurosci. *18*, 1025–1033.

29. Dea, M., Hamadjida, A., Elgbeili, G., Quessy, S., and Dancause, N. (2016). Different patterns of cortical inputs to subregions of the primary motor cortex hand representation in Cebus apella. Cerebr. Cortex *26*, 1747–1761.

30. Hatsopoulos, N., Joshi, J., and O'Leary, J.G. (2004). Decoding continuous and discrete motor behaviors using motor and premotor cortical ensembles. J. Neurophysiol. *92*, 1165–1174.

31. Riehle, A., Grün, S., Diesmann, M., and Aertsen, A. (1997). Spike synchronization and rate modulation differentially involved in motor cortical function. Science *278*, 1950–1953.

32. Arce-McShane, F.I., Hatsopoulos, N.G., Lee, J.-C., Ross, C.F., and Sessle, B.J. (2014). Modulation dynamics in the orofacial sensorimotor cortex during motor skill acquisition. J. Neurosci. *34*, 5985–5997.

33. Flesher, S.N., Downey, J.E., Weiss, J.M., Hughes, C.L., Herrera, A.J., Tyler-Kabara, E.C., Boninger, M.L., Collinger, J.L., and Gaunt, R.A. (2021). A brain-computer interface that evokes tactile sensations improves robotic arm control. Science *372*, 831–836.

STAR★METHODS

KEY RESOURCES TABLE

REAGENT or RESOURCE	SOURCE	IDENTIFIER
Deposited data		
Monkey neural data	This Paper	https://data.mendeley.com/datasets/3b58rk3jp8/draft?a = da69fe10-5dea-4c8c-8418-acd2901fcdb4
Human neural data	This Paper	https://dabi.loni.usc.edu/dsi/UH3NS107714/J8DVJ0JZA7DY
Experimental models: Organisms/strains		
Bx: *Macaca mulatta*, Chinese origin	University of Texas Health Sciences Center, San Antonio, TX	
Yk: *Macaca mulatta*, Chinese origin	Illinois Institute of Technology, Chicago, IL	
Mk: *Macaca mulatta*, unknown origin	University of Wisconsin, Madison, WI Harlow Primate Lab	
Human subject		
P2: A male subject with spinal cord injury		
Software and algorithms		
Matlab R2021a	Mathworks Inc.	www.mathworks.com
Code	This Paper	https://github.com/nichohat/Propagating-Motor-Cortical-Patterns-of-Excitability-are-Ubiquitous-across-Human-and-non-Human-Primat.git

RESOURCE AVAILABILITY

Lead contact

Further information and requests for resources should be directed to and will be fulfilled by the lead contact, Nicholas G. Hatsopoulos (nicho@uchicago.edu).

Materials availability

This study did not use any reagents.

Data and code availability

- Data

Monkey Data: Mendeley Data: https://data.mendeley.com/datasets/3b58rk3jp8/draft?a=da69fe10-5dea-4c8c-8418-acd2901fcdb4

Human Data: DABI: https://dabi.loni.usc.edu/dsi/UH3NS107714/J8DVJ0JZA7DY

- Code: https://github.com/nichohat/Propagating-Motor-Cortical-Patterns-of-Excitability-are-Ubiquitous-across-Human-and-non-Human-Primat.git

EXPERIMENTAL MODEL AND SUBJECT DETAILS

The surgical and behavioral procedures involved with non-human primates were approved by the University of Chicago Institutional Animal Care and Use Committee and conform to the principles outlined in the Guide for the Care and Use of Laboratory Animals. The human study was conducted under an Investigational Device Exemption from the Food and Drug Administration and approved by Institutional Review Board at the University of Pittsburgh (Pittsburgh, PA), registered at ClinicalTrials.gov NCT01894802).

Behavioral tasks

Three male rhesus (*Macaca Mulatta*) monkeys were trained separately on three different tasks, i.e., planar reaching (Monkey Bx, age: 14 years), tongue protrusion (Monkey Yk, age: 6 years) and isometric pinch (Monkey Mk, age: 15 years). In addition, a human male participant (P2, age: 33 years) performed an isometric wrist extension task.

Behavior-1.Two-dimensional planar reach

Monkey Bx was operantly trained to perform a center-out planar reaching task using a two-link exoskeletal robot (BKIN Technologies). The tool-tip of the robot determined the position of a cursor on a screen, and the animal was able to freely move the robot in the horizontal plane using its right upper limb. A vertical screen facing the animal provided visual feedback by moving a cursor in the vertical plane in correspondence with the animal's horizontal movement of the robot arm. The animal had to hold the cursor on a center target for 1000 ms duration to trigger a peripheral target appearance (GO cue). The animal had to move the cursor to reach the peripheral target to get a juice reward. The radial distance between the center and the peripheral target was 6 cm. The animal had to reach the peripheral target within 3000 ms of its appearance. Monkey Bx reached for two peripheral targets, one at 45° (arm movements away from the body) and another at 225° (arm movements toward the body) on a circle of radius 6 cm (where 0° corresponded to rightward movements and 180° corresponded to leftward movements). The choice of target directions was based on the observation that movement paths were generally straighter and were less variable across trials for these target directions. The analog kinematics signals were sampled at 2 kHz throughout the experiment.

Behavior-2.Tongue protrusion task

The animal (Monkey Yk) learned to protrude its tongue onto a strain gauge (Revere Transducers, Mode 462D3-2-10P1R, Tustin) placed in front of the mouth and apply an isometric force at the level cued by target positions. The details are further described in a previous study.[32] The monkey was seated in front of a computer screen that displayed the targets and a cursor that was displaced in proportion to the amplitude of tongue-protrusive force applied on the transducer (sampled at 1 kHz). At the beginning of each trial, a baseline target appeared after a random delay between 750 and 1250 ms. The animal was required to apply a minimal force of ~15 g to reach a baseline target and hold for a random period of 500–1000 ms. Subsequently, at the end of the hold period, a new target appeared whose position was determined by the instructed force ranging between 50 and 80 g. Upon successful hitting of the target within a time window of 5000 ms, a juice reward was dispensed. A 3000 ms inter-trial interval was observed in the experiments.

Behavior-3. Isometric pinch

One adult male rhesus macaque (Monkey Mk) participated in the experiment. The animal was trained to sit in a primate chair with forearm restrained by a well-padded arm rest mounted on a table in front of him, and apply an isometric pinch force using the thumb and index fingers. At the beginning of each trial, a baseline target appeared. The animal was required to apply a minimal force to reach a baseline target, and upon reaching the baseline target, a final target appeared. The animal applied a pinch force to drive a cursor toward the final target for a reward. A time limit of 3000 ms was enforced for the animal to reach the target. A padded elbow block prevented elbow rotation. The digits of the animal made contact with a custom fixture to measure pinch force. Two subminiature load cells (ML13, 1 Kg, Honeywell, Columbus, OH) embedded in the fixture measured the index and thumb isometric pinch force individually. All of the remaining joints of the index finger and thumb were fixed at angles appropriate for palmar pinch with a plastic splint.

Behavior-4 isometric wrist extension

A male, human participant (P2) performed the wrist extension under isometric conditions by applying a force to a strain gauge positioned against the back of the pronated hand. The participant had tetraplegia due to a C5 motor/C6 sensory ASIA B spinal cord injury. The injury was sustained about 10 years before participation in the clinical trial, which began when he was 28 years old. Additional details regarding his implant can found in previous studies[33] that occurred prior to the experiments presented here. The participant has no volitional movement of his fingers, but retains some limited wrist extension strength, as well as more proximal arm function. At the beginning of each trial, the subject was instructed about one of the two force levels based on percentages of maximum voluntary contraction. After an instructed delay of 2000 ms,

a chime was presented as the GO cue to initiate wrist extension. A strain gauge translated the applied force into proportional displacement of a cursor on the screen. The analog force signal was sampled at 1 kHz.

Electrophysiology

Non-human primate subjects

All the subjects were implanted with at least one array of electrodes (Blackrock Neurotech, Inc. Salt Lake City, UT) in the relevant primary motor area. Monkey Bx (planar reach) was implanted with two arrays with 64 recording electrodes per array (8 × 8 grid; 1.5 mm depth; 400 μm pitch), positioned on the precentral gyrus along the medio-lateral axis. Only the medial array that corresponded to upper limb area of the M1 was used for the analyses. Monkey Mk (isometric pinch) was implanted with one array of 100 electrodes (10 × 10 grid; 1.0 mm depth; 400 μm pitch) in the M1 contralateral to the hand used for behavior. A second array had been implanted in M1 of Mk, but the connector was explanted by the time the experiment took place. Two 100-electrode arrays (10 × 10 grid; 1.5 mm depth; 400 μm pitch) were implanted in the M1 and S1 orofacial regions of the Monkey Yk (tongue protrusion). Only data from the M1 implant was analyzed for this study.

Surface electrical stimulation during surgical implantation was performed to guide the placement of each electrode array in the arm/hand or orofacial area of primary motor cortex.

Neural data recorded as analog signals were amplified with a gain of 5000, bandpass filtered between 0.3Hz and 7.5 kHz, and digitized at 30 kHz. For Bx, the local field potentials were zero-phase low-pass filtered with a 10^{th} order Butterworth filter and a cut-off frequency of 500 Hz, and down-sampled to 2 kHz. For monkeys Yk and Mk, the local field potentials were sampled at 1 kHz and 2 kHz, respectively, from the digitized data after low-pass filtering the signals with a fourth order Butterworth filter and a cut-off frequency of 500 Hz.

Human participant

The human participant received two arrays in M1 and two in S1. Data from the lateral array in M1 was used here as it is expected to respond to wrist and finger movements. The array had 100 electrodes (10 x 10 grid; 1.5 mm and 400 μm pitch), and a NeuroPort data acquisition system (Blackrock Neurotech, Inc.) was used to record the neural data. The LFPs were sampled at 1 kHz after digitization and filtering. The participant provided informed consent prior to performing any study-related procedures.

METHOD DETAILS

Beta band and single-trial beta attenuation orientation

The channel-averaged power spectral density was computed for the neural signals from each array over a large number of trials, and the peak beta frequency (in the range of 15–35 Hz) was estimated for each animal and the human subject. For monkeys Bx and Mk the beta peak occurred at 31 Hz, and for monkey Yk, the peak occurred at 23 Hz (approximated to the nearest integer value). The beta peak for the human subject was estimated as 30 Hz. The signal was then band-pass filtered with a bandwidth of 6 Hz centered on the frequency at peak beta, i.e., 31 $\pm$ 3 Hz (Bx and Mk), 23 $\pm$ 3 Hz (Yk) and 30 $\pm$ 3 Hz (HN). A zero-phase implementation of the band-pass filter was used to filter the signal concurrently from all the electrodes. This ensured that the filter did not affect the phase relationship across the electrodes and in addition, did not introduce any phase shifts. The beta envelopes of the signal were computed using the magnitude of the Hilbert transformation applied to the band-pass filtered signal.

An auto-encoder neural network, previously described in,[1] was used to extract the single-trial beta envelopes. A segment of the signal (−500 to 600 ms for Bx, −1000 to 1500 ms for Yk, and −1000 to 1000 ms for the human subject, with respect to GO cue; −1000 to 250 ms for Mk with respect to the movement onset) served as the input for the auto-encoder. The extracted data were decimated to 100 Hz before training the neural network. A vector of length nChannels × mSamples was created for each trial and fed through the auto-encoder. With training, the auto-encoder was able to reconstruct the signal that preserved both spatial patterns and significant temporal variance of the signal. The output beta envelopes from the auto-encoder were then low-pass filtered with a 10^{th} order filter and cut-off frequency of 5 Hz. The filtered signals were normalized to have an amplitude range of [0, 1], and resampled to their original sampling rate.

The normalized single-trial beta envelope attenuated and crossed an amplitude threshold value at a particular time (referred to as beta attenuation time or BAT) which varied depending on the channel (see Figure 1 middle row). These BATs, when arranged spatially on their corresponding electrode locations on the array, exhibited a propagating pattern with a particular orientation. The orientation of the beta attenuation (BAO) was estimated using a linear regression fit to the BATs as follows,

$$\widehat{BAT}_{rc} = \beta_r r + \beta_c c + \alpha \quad \text{(Equation 1)}$$

where, β_r and β_c are the coefficients of the rows and columns of the array, and α denotes the constant offset time. The direction of BAO was then estimated as,

$$\widehat{BAO} = \arctan\left(\frac{\beta_r}{\beta_c}\right) \quad \text{(Equation 2)}$$

The F-statistic of the model was used to ascertain statistical significance of the fit. For each trial, a BAO and its associated coefficient of determination (R^2) were calculated. On any given trial, the amplitude threshold for determining the BATs was determined by varying the amplitude from 0.7 to 0.15 (0.5 to 0.15 for Bx) in steps of 0.05 and finding the threshold with the largest associated R^2.

Computing propagation speed

Using the estimated BAT ($\widehat{BAT}$) for each electrode in a trial and the electrode spacing (400 μm for all the arrays), a time gradient was computed across the grid. The inverse of the magnitude of the gradient gave the speed of propagation of beta attenuation.

Computing response times of single trials

For reaching behavior, the tangential velocity trajectories estimated from the Cartesian position of the reaching kinematics data sampled at 2 kHz were used to compute the response time. From the normalized trajectories of each trial, movement onset times were computed when the velocity crossed 10% of the peak velocity. When there were smaller velocity peaks that exceeded the 10% threshold prior to final velocity peak associated with the actual movement to the target, movement onset was computed using the final threshold crossing. Likewise, for the behaviors involving force, a normalized force profile was used. The force data were sampled at 2 kHz for the tongue and pinch behaviors and at 1 kHz for the human wrist extension trials. For the tongue task, the time at which the applied force exceeded a defined threshold (1 g) prior to reaching two-thirds of peak force was used as the force onset time.[32] The time at which the force level reached a 10% of the peak force was used as force onset time for the pinch and the human wrist extension behavior (See Data S4 for distributions of response times).

Shuffling analysis

As an additional method for assessing significance of linear propagation, a shuffling analysis was used to determine a significance threshold for R^2 when fitting BATs to a plane. A set of 100 trials were randomly chosen per task and a planar fit was computed on the BATs with electrode locations shuffled. This was repeated a 1000 times with the same 100 trials yielding a distribution of R^2 values (see Data S2). The threshold value for R^2 was set at 5%, and any single trial with R^2 greater than the threshold was included in further analyses. For monkey Mk, the trials chosen for shuffling were 79 instead of 100. And, for Monkey Bx, the R^2 cutoff was retained at 0.2, as in a previously published study.[1]

QUANTIFICATION AND STATISTICAL ANALYSIS

Throughout this paper, a statistical test was deemed significant when the resulting p value was lower than 0.05, unless otherwise noted. Details about the specific statistical test, sample number, and any post-hoc corrections can be found in the results section and in the corresponding figure captions.

ADDITIONAL RESOURCES

The human study was conducted under an Investigational Device Exemption from the Food and Drug Administration and approved by the Institutional Review Board at the University of Pittsburgh (Pittsburgh, PA), registered at ClinicalTrials.gov (NCT01894802).